Microscale coiling in bis-imidazolium supramolecular hydrogel fibres induced by release of a cationic serine protease inhibitor

David Limón,[a,b] Claire Jiménez-Newman,[a] Ana C. Calpena,[b,c] Arántzazu González-Campo,[d] David B. Amabilino,[e,f] and Lluïsa Pérez-García.[a,b,‡,*]

a. Departament de Farmacologia, Toxicologia i Química Terapèutica, Universitat de Barcelona, Av. Joan XXIII, 27-31, 08028 Barcelona, Spain.

b. Institut de Nanociència i Nanotecnologia IN2UB, Universitat de Barcelona, 08028 Barcelona, Spain.

c. Departament de Farmàcia, Tecnologia Farmacèutica i Fisicoquímica, Universitat de Barcelona, Av. Joan XXIII, 27-31, 08028 Barcelona, Spain.

d. Institut de Ciència de Materials de Barcelona (ICMAB-CSIC). Campus de la UAB, 08193, Bellaterra, Barcelona, Spain.

e. School of Chemistry, University of Nottingham, University Park, NG7 2RD, United Kingdom.

f. The GSK Carbon Neutral Laboratories for Sustainable Chemistry, The University of Nottingham, Triumph Road, Nottingham NG7 2TU, United Kingdom.

**Corresponding author. Email: mlperez@ub.edu*

‡ Present address: School of Pharmacy, The University of Nottingham, University Park, Nottingham NG7 2RD, England, United Kingdom.

ABSTRACT

Gels formed by a gemini dicationic amphiphile incorporate a serine protease inhibitor, which could be used in a new approach to the treatment of Rosacea, within the fibres as well as in the space between them, affecting a number of gel properties but most importantly inducing remarkable fibre coiling at the microscopic level as a result of drug release from the gel. Drug release and skin permeation experiments show its potential for topical administration.

INTRODUCTION

Low molecular weight gelators (LMWGs) self-assemble to form fibres through non-covalent forces.[1] These supramolecular gels are soft and sometimes thermoreversible, making them suitable for therapeutic applications.[2] Their three-dimensional morphology depends on the nature of the gelator, the self-assembly conditions, and non-covalent interactions established with host molecules incorporated into the gel matrix, like, ion-dipole interactions in metal and anion-binding gels.[3] Also, gel skeletal modification can be made introducing metal ions.[4]

However, to the best of our knowledge, no examples are known of changes in the morphology of the gel fibres caused by the release of a previously incorporated host.

Our group has shown that gemini imidazolium salts can deliver anionic drugs,[5] including from hydrogels that are useful for topical applications.[6] The self-assembly of the cationic gelators and the interaction with anionic guests in the supramolecular gels is driven not only by ionic interactions but also hydrogen bonds and hydrophobic forces.[6] Here, we show that the incorporated drug can also be cationic, that this feature makes drug release more effective, leading to a change in the morphology of the cationic gels through coiling of the gel fibres.

RESULTS AND DISCUSSION

We chose the drug 4-(2-aminoethyl)-benzenesulfonyl fluoride hydrochloride (**AEBSF·HCl**), as an irreversible serine protease inhibitor whose activity has shown to be successful, inhibiting Kallikrein-5 (K5),[7] a protein that is overexpressed in ailments such as Rosacea.[8] Its clinical use would imply a new therapeutic strategy that has not been reported, the main drawback being low drugability. A delivery material could overcome this obstacle and make a novel approach in the topical treatment of Rosacea. Furthermore, topical administration helps increase the drug concentration at the target site, lowering the side effects in other tissues.

For all these reasons, the ability of bis-imidazolium **1·2Br** to form gels in presence of **AEBSF·HCl** (Fig. 1) using water and ethanol as solvents was explored and the gelling conditions were optimized. The structure and behaviour of the gels were characterized, and drug release and skin permeation experiments were performed in order to assess their suitability as a possible new topical treatment for Rosacea.

The optimum gelling conditions of compound **1·2Br** are a final concentration of 5 mg/mL in 50:50 ethanol:water, and at room temperature, giving a fast gel formation (*ca.* 10 min.). The influence of **AEBSF·HCl** concentration was assessed using these optimized conditions. Gels **1·AEBSF** are also formed in 10 minutes in the presence of low concentrations of drug, but the gelling time increased significantly at higher concentrations (above 4 mg/mL, See SI Fig. S1). A final concentration of 5 mg/mL **AEBSF·HCl** was chosen as optimum for being the highest one that permits gelation in 20 minutes or less. This proportion is an approximate 1:4 gelator:drug molar ratio, a much higher loading than that possible using the same gelator and anionic drugs.[6]

Rheological studies of gels **1·2Br** and **1·AEBSF** show their resistance to rupture by the critical stress value: the addition of **AEBSF·HCl** makes the gel three times more elastic as compared to the gel alone (SI Table S1 and Fig. S2), as opposed to the observations with other drugs.[6b] However, when the critical stress is reached, gels show an abrupt rupture rather than a slow one, making it suitable for a topical pharmaceutical form. Frequency sweep tests showed the gel resistance to deformation at different frequencies, shown by the Storage (G') and Loss (G'') moduli, at a constant shear stress of τ = 0.5 Pa for being within the viscoelastic region. In both the gel **1·AEBSF** and the gel **1·2Br**, independently of the frequency applied, an elastic plateau was observed, where the Storage modulus is higher than the Loss modulus (G' >

G''), meaning that gels present a predominant elastic, solid-like behaviour, for which they can be classified as "solid-like" gels.[1a,9] The addition of **AEBSF·HCl** decreases the gel resistance to deformation, making it softer than gel **1·2Br** which is also useful for topical application (SI Fig. S2).

^{1}H NMR spectroscopy experiments show (SI Fig. S3) that at a 1:1 molar ratio of **1·2Br** and **AEBSF·HCl** (5:1 mg/mL) the totality of **1·2Br** assembles forming the gel **1·AEBSF**, leaving no remaining compound in solution, as no peaks from compound **1·2Br** can be observed. *Ca*. 76% of the **AEBSF·HCl** present in the mixture is incorporated in the gel fibres, the remainder left in the interstitial space. The versatility of the gelator **1·2Br** to incorporate both anionic and cationic drugs confirms its promise for drug delivery.

Xerogel **1·2Br** has fibres longer than 20 μm and around 100 nm width, that stick together forming ribbons and do not show signs of ageing (Fig. 2a and Fig. S4a in SI). Contrastingly, the morphology of the gels **1·AEBSF** changes with time, a phenomenon which is also dependent on the concentration of **AEBSF·HCl** used (ranging from 1-5 mg/mL). **AEBSF** precipitates might be expected after complete evaporation of the solvent in the gel, because even at 1 mg/mL 24% of the material is in the interstitial space (as shown by NMR); pure **AEBSF·HCl** precipitates in rod-shaped crystals (Fig. 2b). In all gels with **1·AEBSF**, no clear drug precipitates were found on freshly prepared gels, when gelation takes place in the presence of either 1, 3 or 5 mg/mL of **AEBSF·HCl**, as shown by SEM images (Fig. 2c and SI Fig. S5). It is interesting that fibres in **1·AEBSF** are densely twisted much more than pure gel **1·2Br**, which could be the reason of their subsequent coiling in order to reduce the tension created.

When gels **1·AEBSF** are left for two weeks in a sealed vial the morphology of the xerogels exhibits changes depending of the amount of **AEBSF·HCl** present in the gelation process. Thus, when 1mg/mL of **AEBSF·HCl** was used, the fibres in **1·AEBSF** retain the same morphology as when freshly prepared, as seen in Fig. 2d (see also SI Fig. S5a). In contrast, in the two-week old gels formed at a concentration above 3 mg/mL of **AEBSF·HCl**, the bending of the fibres in a circular way, resembling "coiled ropes" can be observed (Fig. 2d, SI Fig. S4b, Fig. S5a). These rolls range from 5 to 15 μm in diameter, and the thickness of the ring varies widely due to the number of times the "rope" is coiled. As can be seen, the concentration of **AEBSF·HCl** influences the structure of fibres in two-week old gels **1·AEBSF**. Coils were formed both at 3 and 5 mg/mL gels, the coils being thinner at 3 mg/mL, as fibres are coiled less times. Also, at this concentration some long straight fibres are still starting to bend, suggesting the subsequent coil formation.

Just a few examples of differences in morphology of nanostructured materials have been reported before,[10] but mainly as the consequence of induced self-assembly after evaporation, and very rarely as a result of doping gels with metal ions.[4] The coiling observed on the fibres of **1·AEBSF** appears as an unprecedented example of ordering rearrangement induced by intermolecular interactions. Thus, the cationic drug **AEBSF·HCl** seems to be kinetically entrapped within the gel nanostructure, due to the fast self-assembly in the gelation process, generating a metastable state where the drug is incorporated in the lamellar gel.

However, its presence disturbs the interlayer packing of the gelator **1·2Br** that can experiment alterations upon changes in external experimental conditions.

The chemical composition of the fibres was measured by Energy Dispersive X-ray spectroscopy (EDX) on different areas of two-week old **1·AEBSF** xerogels assembled in the presence of 3 mg/mL (SI Fig. S6) or 5 mg/mL (Fig. 3) of **AEBSF·HCl**. The spectra show the presence of sulphur in the straight fibres in gels for both concentrations, confirming the presence of the drug after two weeks. However, in the coiled fibres the absence or diminution of both the sulphur and fluorine peaks suggests that there is release of drug from the fibres over time, presumably into the interstitial liquid. The release could trigger the disruption in the interlayer packing within the fibres, prompting their coiling.

Differential Scanning Calorimetry (DSC) showed that the time needed for gel formation of **1·AEBSF** and the thermodyna mic parameters associated with the phase transition are very different to gel **1·2Br**. The addition of **AEBSF·HCl** to gelator **1·2Br** influences greatly the gelling temperature (Fig. S7 in SI), time of gelation, and associated enthalpy change. Gel **1·2Br** spontaneously starts forming at around 21 °C, while gel **1·AEBSF** starts forming at *ca.* 30 °C. This shows that adding the drug makes the gel more stable at higher temperatures. Conversely, the whole width of the peak indicates the total time for gel formation, which increases considerably from around 5 min to 20 min by adding **AEBSF·HCl**, similar to the observations with the naked eye, and suggesting that the interaction between the drug and the gelator lengthens the gelling period, presumably because of slower gel fibre assembly. The heat capacity (C_p) in the plot also represents the speed of gelation, where the onset temperature is the point at which gelation starts, and the maximum value is when the gelation occurs fastest. For instance, the gelation of **1·AEBSF** is 20 times slower than that of gel **1·2Br**, which is in accordance to the increase in the gelling period.

The most noticeable change observed is in the thermodynamic parameters of the process. The gelation of **1·2Br** is exothermic, and is related to the decrease of entropy upon the formation of fibres. Very differently, the gelling of **1·AEBSF** shows both an exothermic event in the beginning, and an endothermic one at lower temperatures, giving an overall enthalpy close to zero. These results indicate that upon the mixture of **1·2Br** with **AEBSF·HCl** and the solvents, not only the gelation occurs, but at least a second process is happening at the same time, which is endothermic, and therefore, necessarily entropic. This event could be an adsorption of the drug in the interstitial space of the gel to the fibres, and might be related to an increase in the surface tension of the solvent. The thermoreversibility of **1·AEBSF** was proven by subsequent heating-cooling cycles, in order to melt the gel and form it again, and similar peaks were observed. However, a slight decrease in C_p values, and a slight increase in the gelling temperature, occur in each cycle, which suggests that heating up the sample to 35 °C melts the gel but still leaves some gel nucleation points intact, not seen macroscopically, which facilitate the subsequent gelation on cooling (SI, Table S2 and Fig. S8).

Drug release experiments from the nanocomposite material using PBS as the receptor medium for complying SINK conditions,[11] to prove of the drug when applied on human skin is not limited, showed that gel **1·AEBSF** releases almost 92% of the drug during the first 15 hours

(fitting a one phase exponential association model). Afterwards, drug degradation occurs in the receptor chamber,[12] following a one phase exponential decay model (Fig. 4 and Table S3). This degradation would not compromise the therapeutical efficacy of the gel when applied on the skin, as the speed of release is ten times higher than the speed of degradation, whose half-life (55 h) is much longer than the usual administration intervals of topical formulations. Moreover, at the normal pH of the skin (5.5), degradation would barely occur. Permeation studies on human skin show that **1·AEBSF** promotes the complete permeation of **AEBSF** through the skin in 6 hours (lag-time, see Fig. 5 and SI Table S4). As K5 is located mainly at the epidermis, specifically at the cornified and granular layers,[13,14] the amount of drug retained inside the skin becomes an even more important parameter to be considered. The total amount of **AEBSF** retained (A_s corr.) is estimated by considering both the amount of drug extracted from the skin after the experiment [A_s] and the percentage of drug that can actually be extracted out of the total drug retained (recovery experiments). After topical application, around 3484 $\mu g/g \cdot cm^2$, is retained in the skin, where it has its therapeutic activity, equivalent to 69% of the total dose applied (Fig. 5).

Changes in the morphology of the gels were scrutinized by SEM after being subjected to release conditions, for a maximum of 16 h, the maximum period permitting almost a total release with no detectable hydrolysis of the drug. In all the samples, some lumpy material arises from the buffer used under those conditions. No variation was observed for the pure gel **1·2Br**, for which only straight fibres were seen (Fig. S9 in SI). The release of the drug from **1·AEBSF** under these release conditions for 6 and 16 hours is also accompanied by the formation of fibre coils (see SEM images in SI Fig S9 and S10). The images clearly show the formation of coils and a more structured and curved nature to the fibres of the gelator. Direct quantification is not possible, but the number of coiled fibres seems similar to those on aged gels under storage conditions over a longer period of time. While the morphological change is clear, powder X-ray diffraction of gels before and after release shows no significant structural rearrangement (Fig. S11 in SI). A model such that in Fig. S12 might explain this observation.

In summary, **AEBSF·HCl** strongly influences the self-assembly of **1·2Br** and the behaviour of the resulting gel, which is soft and thus suitable for dermal application. **AEBSF** is released from the gel, triggering its morphological change evidenced by the twisting of fibres and the subsequent formation of coils, although not all fibres are able to coil, presumably because their length and being trapped physically by other fibres. Almost all the drug incorporated in **1·AEBSF** is released and penetrates human skin, where it is retained. By the nature of the drug incorporated, this gel would imply a novel therapeutic approach in the topical treatment of ailments like Rosacea.

Acknowledgements: Financial support was from the MINECO (Projects TEC2014-51940-C2-2-R, MAT2013-47869-C4-2-P and SEV-2015-0496). We thank Dr. Lyda Halbaut (UB) for help with rheology studies. D.L. thanks CONACYT for a predoctoral grant.

References

1. (a) K. J. Skilling, F. Citossi, T. D. Bradshaw, M. Ashford, B. Kellam and M. Marlow, *Soft Matter*, 2014, **10**, 237-256; (b) D. Yuan and B. Xu, *J. Mater. Chem. B*, 2016, **4**, 5638-5649.

2. (a) A. Vashist, A. Vashist, Y. K. Gupta and S. Ahmad, *J. Mater. Chem. B*, 2014, **2**, 147-166; (b) K. J. Skilling, B. Kellam, M. Ashford, T. D. Bradshaw and M. Marlow, *Soft Matter*, 2016, **12**, 8950-8957; (c) J. Shen, L. Song, X. Xin, D. Wu, S. Wang, R. Chen and G. Xu, *Colloid Surface A*, 2016, **509**, 512-520.

3. M.-O. M. Piepenbrock, G. O. Lloyd, N. Clarke and J. N. Steed, *Chem. Rev*., 2010, **110**, 1960-2004.

4. P. Xue, H. Wu, X. Wang, T. He, R. Shen, F. Yue, J. Wang and Y. Zhang, *Sci. Rep*., 2016, **6**, 25390-25396.

5. (a) L. Casal-Dujat, P. C. Griffiths, C. Rodríguez-Abreu, C. Solans, S. Rogers and L. Pérez-García, *J. Mater. Chem. B*, 2013, **1**, 4963–4971; (b) L. Casal-Dujat, M. Rodrigues, A. Yagüe, A. C. Calpena, D. B. Amabilino, J. González-Linares, M. Borràs and L. Pérez-García, *Langmuir*, 2012, **28**, 2368–2381; (c) M. Rodrigues, A. C. Calpena, D. B. Amabilino, D. Ramos-López, J. de Lapuente and L. Pérez-García, *RSC Adv.*, 2014, **4**, 9279–9287; (d) E. Amirthalingam, M. Rodrigues, L. Casal-Dujat, A. C. Calpena, D. B. Amabilino, D. Ramos-López and L. Pérez-García, *J. Colloid Interface Sci.*, 2015, **437**, 132–139.

6. (a) M. Rodrigues, A. C. Calpena, D. B. Amabilino, M. L. Garduño-Ramírez and L. Pérez-García, *J. Mater. Chem. B*, 2014, **2**, 5419-5429; (b) D. Limón, E. Amirthalingam, M. Rodrigues, L. Halbaut, B. Andrade, M. L. Garduño-Ramírez, D.B. Amabilino, L. Pérez-García and A. C. Calpena, *Eur. J. Pharm. Biopharm.*, 2015, **96**, 421–436.

7. K. Yamasaki, J. Schauber, A. Coda, H. Lin, R. A. Dorschner, N. M. Schechter, C. Bonnart, P. Descargues, A. Hovnanian, and Richard L. Gallo, *FASEB J*., 2006, **20**, 2068–2080.

8. (a) K. Yamasaki, A. Di Nardo, A. Bardan, M. Murakami, T. Ohtake, A. Coda, R. A. Dorschner, C. Bonnart, P. Descargues, A. Hovnanian, V. B. Morhenn and R. L. Gallo, *Nat Med*, 2007, **13**, 975–980; (b) K. Yamasaki and R. L. Gallo, *J. Investig. Dermatology Symp. Proc.*, 2011, **15**, 12–15.

9. M. A. Rogers and J. H. J. Kim, *Food Res. Int.*, 2011, **44**, 1447–1451.

10. (a)L. Wan, L. Li and G. Mao, *Nanoscale Res. Lett*., 2011, **6**, 49-56; (b) M. Wang, A. R. Mohebbi, Y. Sun and F. Wudl, *Angew. Chem. Int. Ed*., 2012, **51**, 6920-6924; (c) B. Li, J. Puigmartí-Luis, A. M. Jonas, D. B. Amabilino and S. De Feyter, *Chem. Commun*., 2014, **50**, 1326-13219.

11. M. Gibaldi and S. Feldman, *J. Pharm. Sci.*, 1967, **56**, 1238–1242.

12. G. R. Mintz, *BioPharm*, 1993, **6**, 34–38.

13. M. Miyai, Y. Matsumoto, H. Yamanishi, M. Yamamoto-Tanaka, R. Tsuboi and T. Hibino, *J. Invest. Dermatol.*, 2014, **134**, 1665–74.

14. M. Brattsand and T. Egelrud, *J. Biol. Chem.*, 1999, **274**, 30033–30040.

Figures

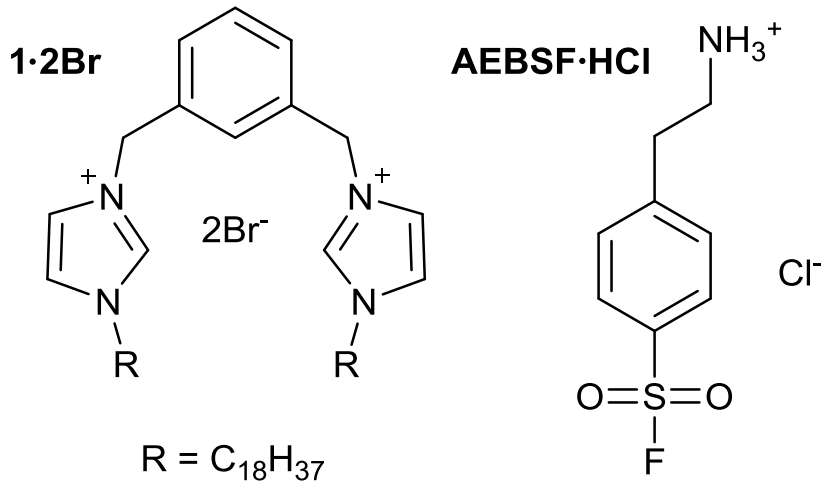

Fig. 1 Chemical structures of the gelator **1·2Br** and the serine protease inhibitor **AEBSF·HCl**.

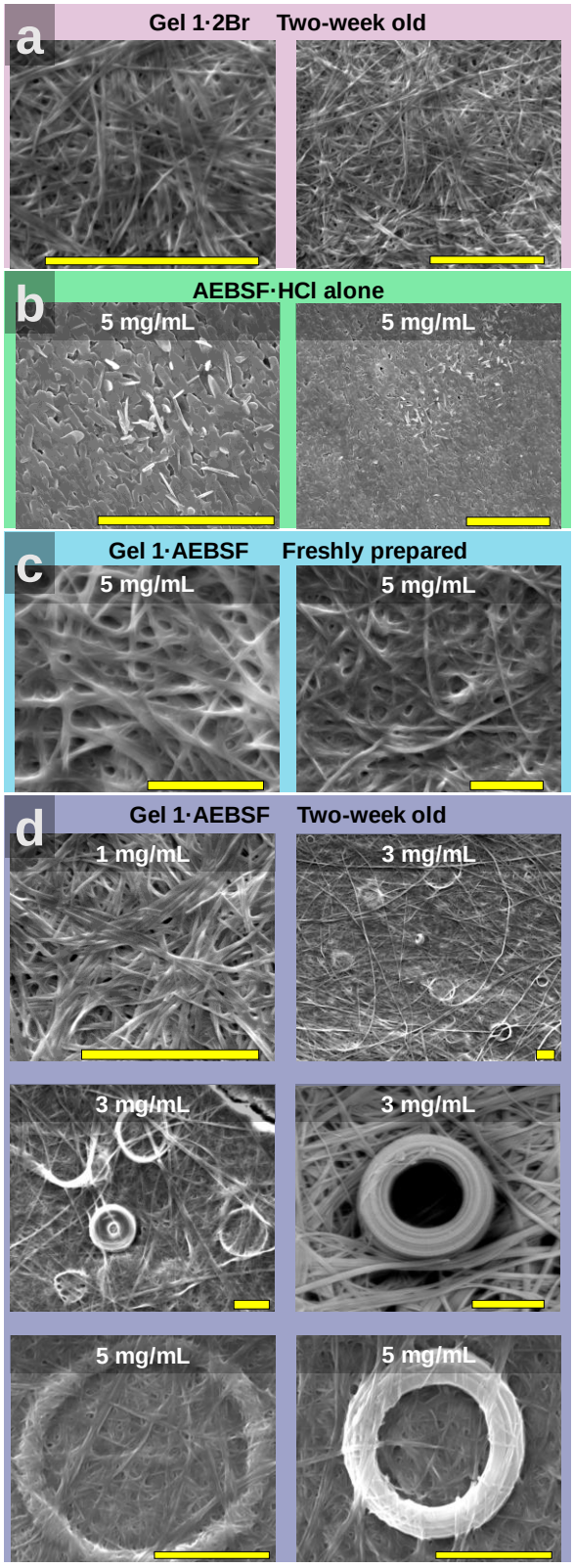

Fig. 2 SEM images showing the influence of drug concentration and age of the gel on the morphology of gel fibres. a) Gel **1·2Br**. b) Precipitates of **AEBSF·HCl**, from a 5 mg/mL solution. c) Freshly prepared **1·AEBSF** gel. d) Influence of the drug concentration in a two-week old gel. Yellow scale bar represents 8 µm in all images.

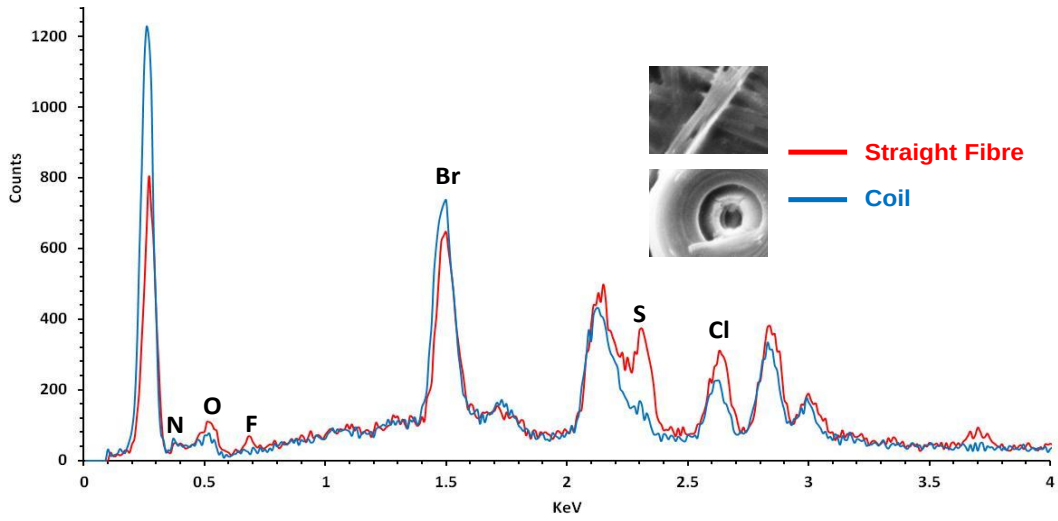

Fig. 3 EDX spectra from straight fibre and coiled fibre of 5 mg/mL **1·AEBSF** gel.

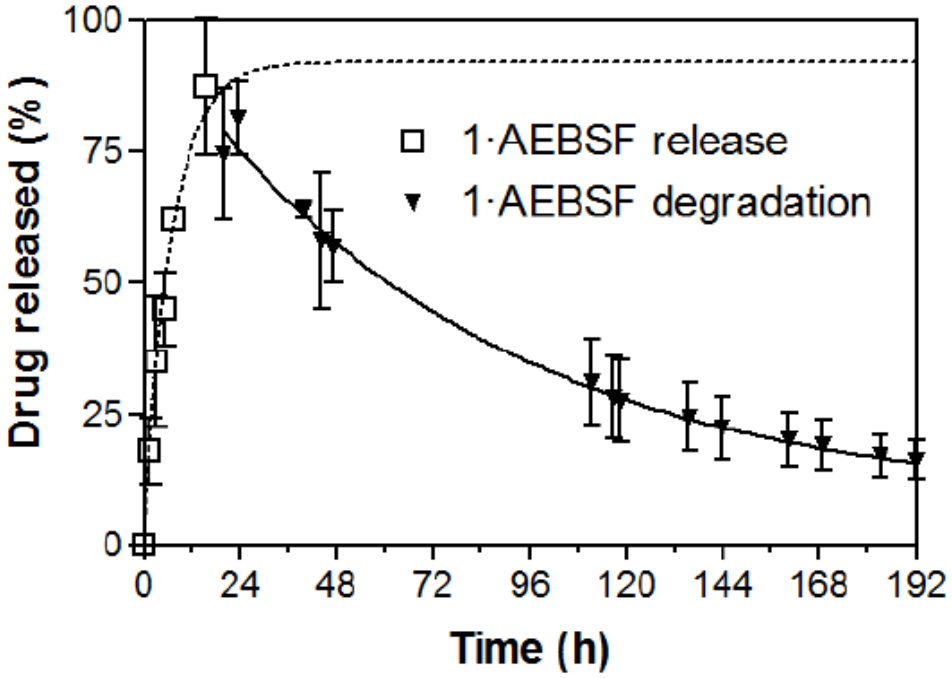

Fig. 4. Cumulative amount of drug released of from gel **1·AEBSF** and degradation in receptor medium. Values are means and error bars represent one standard deviation (n=3). Release and decay both follow one phase exponentials (see ESI and equation parameters in **Table S3**).

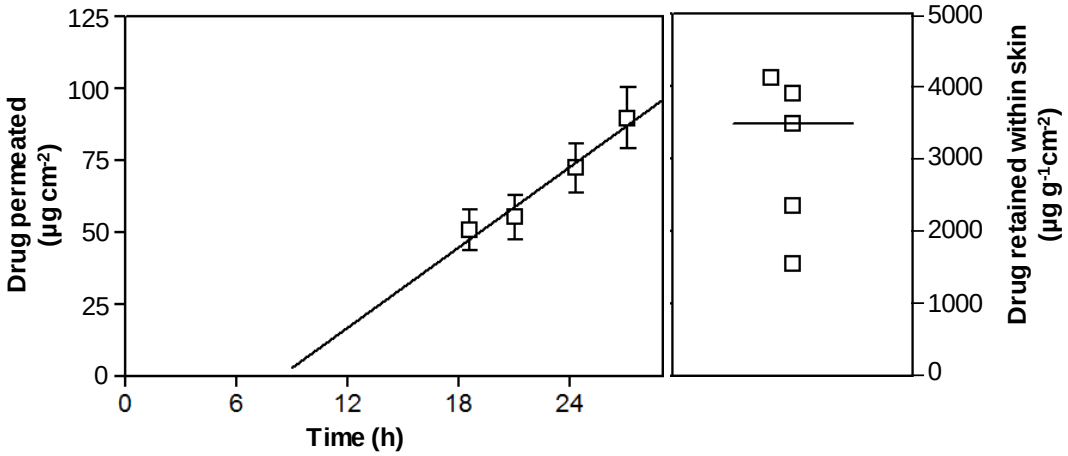

Fig. 5. Cumulative amount of **AEBSF** permeated (left) and retained in human skin (right) after application of gel **1·AEBSF.** Values in permeation experiments represent the Means ± one standard deviation. The bar in retention experiments represents the Median value (n=5).

SUPPLEMENTARY INFORMATION

Microscale coiling in bis-imidazolium supramolecular hydrogel fibres induced by release of a cationic serine protease inhibitor

David Limón,[a,b] Claire Jiménez-Newman,[a] Ana C. Calpena,[b,c] Arántzazu González-Campo,[d] David B. Amabilino,[e,f] and Lluïsa Pérez-García.[a,b,δ,]*

[a]Departament de Farmacologia, Toxicologia i Química Terapèutica, Universitat de Barcelona, Av. Joan XXIII, 27-31, 08028 Barcelona, Spain.

[b]Institut de Nanociència i Nanotecnologia IN2UB, Universitat de Barcelona, 08028 Barcelona, Spain.

[c]Departament de Farmàcia, Tecnologia Farmacèutica i Fisicoquímica, Universitat de Barcelona, Av. Joan XXIII, 27-31, 08028 Barcelona, Spain.

[d]Institut de Ciència de Materials de Barcelona (ICMAB-CSIC). Campus de la UAB, 08193, Bellaterra, Barcelona, Spain.

[e]School of Chemistry, University of Nottingham, University Park, NG7 2RD, United Kingdom.

[f]The GSK Carbon Neutral Laboratories for Sustainable Chemistry, The University of Nottingham, Triumph Road, Nottingham NG7 2TU, United Kingdom.

[δ]Present address: School of Pharmacy, The University of Nottingham, University Park, Nottingham NG7 2RD, England, United Kingdom.

*Corresponding author. Email: mlperez@ub.edu

TABLE OF CONTENTS

EXPERIMENTAL SECTION

Materials

All reagents were of analytical grade. 4-(2-aminoethyl)benzenesulfonyl fluoride hydrochloride (**AEBSF·HCl**) was purchased from Fisher Scientific. Phosphate buffered saline and Ethanol HPLC grade were purchased from Sigma-Aldrich. Water was obtained from a MilliQ equipment from Millipore®.

Synthesis

Compound 1,3-bis[(3-octadecyl-1-imidazolio)methyl]benzene dibromide (**1·2Br**) was prepared as reported previously.[1]

Methods

Gel preparation

Gels were always prepared by dissolving compound **1·2Br** in ethanol, adding distilled water as the anti-solvent, mixing gently and storing without disturbance in closed vials to prevent solvent evaporation.

Influence of drug concentration on gel formation

Solubility of **AEBSF·HCl** was previously assessed in water in order to determine the drug concentrations in gel to be assayed. For the gels with **1·2Br** and **AEBSF·HCl** 10 mg of the gelator was dissolved in 1 mL of ethanol. 1 mL of an aqueous solution containing different amounts of drug (1, 2.5, 3.5, 5, 10, 20 and 40 mg) was added and the solution was gently stirred and left to stand at room temperature as described above.

Optimum conditions for gel fabrication

Optimum conditions were chosen for the preparation of gels, which were used in the rest of the experiments either with or without drug, unless stated otherwise. For instance, the final volume was 2 mL, with a final concentration of 1·2Br of 5 mg/mL as the gelator molecule, using a proportion of 50% ethanol and 50% water, and both mixing and storing at room temperature. Concentration of **AEBSF·HCl** was 5 mg/mL unless differently stated for being the highest that presents no problems for gelling, except for SEM images in which three different concentrations were used, and drug incorporation studies (NMR), in which the molar ratio gelator:drug was 1:1. Gelator **1·2Br** was dissolved in ethanol and was mixed with the drug solution in water. Samples were mixed gently, closed for preventing solvent evaporation, and left to stand without disturbance.

Gel characterization

Rheology Experiments

Rheological studies of gels **1·2Br** and **1·AEBSF** were performed in order to know their viscoelastic behaviour. Amplitude sweep tests show their resistance to rupture by the critical stress value.

For rheological studies, gels were formed in 7 cm diameter glass Petri dishes, forming a total volume of 27 mL. Prepared gels were always kept at room temperature overnight before study.

The rheological characterization was performed using a Haake Rheostress1 rheometer (Thermo Fisher Scientific, Karlsruhe, Germany) connected to a temperature control Thermo Haake Phoenix II + Haake C25P and equipped with parallel plate geometry (Haake PP60 Ti, 60 mm diameter, 3 mm gap between plates).

Oscillation amplitude tests: The amplitude in shear stress τ was increased for 0.01 to 100 Pa with constant frequency of 1 Hz for evaluating the gel strength. Oscillation frequency tests were carried out from 0.01 to 10 Hz at a constant shear stress within the linear viscoelastic region, in order to determine the related variation of storage modulus (G') and loss modulus (G") at 32ºC. Both viscoelastic moduli are defined as follows: $G'=\tau_0/\gamma_0 \cos \delta$ and $G''= \tau_0/\gamma_0 \sin \delta$ (where τ_0 and γ_0 are the amplitudes of stress and strain, and δ is the phase shift between them).

The software Haake RheoWin®Job Manager V.3.3 and RheoWin®Data Manager V.3.3 (Thermo Electron Corporation, Karlsruhe, Germany) were used to carry out the test and analysis of the obtained data, respectively.

Drug incorporation into gel fibres

Incorporation of drug into the gel **1·2Br** was quantified by ^{1}H NMR spectroscopy using a Varian 400 MHz NMR spectrometer from the *Centres Científics I Tecnològics de la Universitat* de Barcelona (CCiT-UB). 32 scans were recorded in every measurement.

For quantifying the incorporation of drug inside the gel fibres, gels from **1·2Br** incorporating drug at a molar ration of 1:1 were formed inside the NMR tube, and the drug signals in spectra were compared to those from a drug solution at the same concentration. Peaks of the aromatic moeity from the drug were taken as the reference signal. For instance, two aliquots containing (8.28 µmol) of **AEBSF·HCl** each were dissolved in 0.75 mL of deuterium oxide and ^{1}H NMR spectra of both (Tubes A and B) were recorded (Record 1). After that, 0.75 mL of deuterated methanol was added to tube A and 7.5 mg (8.28 µmol) of **1·2Br** dissolved in 0.75 mL of deuterated methanol was added to tube B. Both tubes were shaken to promote mixing and the gel formation in tube B was observed, while tube A remained in solution. ^{1}H NMR spectra of both tubes were recorded in the same conditions (Record 2).

Microscopy: SEM/EDX

In all cases, xerogel samples were prepared by completely evaporating the solvent from freshly and two-week old gels.

Scanning Electron Microscopy (SEM) images and EDX analyses were acquired by the Electron Microscopy Service in the Institut de Ciència de Materials de Barcelona – Consejo Superior de Investigaciones Científicas (ICMAB-CSIC) on a QUANTA FEI 200 FEG-ESEM system on samples deposited on carbon tape, dried with N2 .and coated with a layer of gold.

Calorimetric studies

We have used this technique to evaluate the influence that the incorporation of **AEBSF·HCl** in gel **1·AEBSF** has on the temperature and time of gelation, as well as on the changes in thermodynamic parameters such as enthalpy and entropy, as compared to gel **1·2Br**. The strategy consists on introducing the freshly prepared mixture of the gelator, the solvents, and **AEBSF·HCl** if it is the case, into the equipment above the gel's melting temperature. After that, temperature is slowly decreased in order to form the gel inside the equipment, while continuously tracking heat changes. Note that thermograms are plotted in an increasing temperature scale, but experiments are performed by decreasing the temperature, for which plots should be read from right to left.

A Microcal VP-DSC from Mettler-Toledo was used for performing the gelation of compound **1·2Br**. 0.5 mL of a mixture of compound **1·2Br** with both ethanol and water was introduced in the equipment at 35 °C. The sample was then cooled down slowly at 1 °C/min, from 35 °C to 5 °C, in order to form a gel inside the equipment, while monitoring the specific heat capacity (C_p) during the cooling of the sample.

Release studies

Drug release experiments were performed to prove that gel **1·AEBSF** can release **AEBSF·HCl** from the nanocomposite material, and to demonstrate that such profile will not limit the permeation of the drug when applied on human skin. Conditions such as the Franz cells used and the temperature bath at 32 ºC were adjusted to be similar than those in the skin permeation experiments. PBS was chosen as the receptor medium for complying SINK conditions.

Drug release studies from the gels were performed in a Microette transdermal diffusion system (Microette plus-Hanson Research) following previously reported methodologies.[2,3] Vertically assembled Franz-type diffusion cells (Crown Glass) (2.54 cm^2 diffusion area) were used. Dialysis membranes (Cellu·Sep T3 dialysis membrane, MWCO 12000 – 14000 Da, MFPI, USA), previously hydrated in ethanol:water 7:3, were placed in the Franz-type diffusion cells. Receptor chamber contained 10 mM PBS pH 7.4 for the study of gels with **AEBSF·HCl**, complying with SINK conditions.[4] The dialysis membrane and the donor container were put onto the glass receptor chamber and the assembly was fixed with a joint. The Franz-type cells were connected to a controlled temperature circulating bath set to 32°C. Gels of **1·2Br** were prepared at a drug concentration of 5 mg/mL. Known weights of gel were placed into the donor compartment onto the dialysis membranes and the donor compartment was sealed with plastic paraffin film to prevent solvent evaporation. Samples were taken at given time intervals, and every sample taken was replaced by equal volume of the receptor solution. Release experiments of gels were done in triplicate. Concentrations of samples were

determined by HPLC and cumulative amounts of released drug as a function of time were plotted. Kinetic parameters were calculated from the Mean values of three replicas, performing a nonlinear least-squares regression using GraphPad Prism® (version 3.00, GraphPad software, Inc., USA). Different models were tested: Higuchi's square root of time, Korsmeyer-Peppas, One Phase Exponential Assosiation (first-order), Weibull's equation and Zero-order. The best model was chosen accordign to de R^2 value.

Skin permeation studies

The permeation assay was done with human skin from the abdominal region obtained during plastic surgery of a healthy, 40 year-old woman who gave written, informed consent to the use of this material for research purposes. The protocol was similar to that followed in the drug release study, replacing the dialysis membranes with skin previously dermatomed at 0.4 mm thickness, and placed with the stratum corneum facing the donor compartment, according to the guidelines.[5,6] Gel was applied on the donor compartment (408.3±52.7 mg of gel, 2.3±0.3 mg of drug) in contact with the epidermal side of the skin (n=5). The samples were taken at given time intervals for 24 hours. Concentrations were determined using HPLC and cumulative amounts of drug permeated were plotted. Kinetic parameters were calculated from the Median and range values performing a linear least-squares regression in the linear zone of the plot,[7] using GraphPad Prism® (version 3.00, GraphPad software, Inc., USA).

Drug retained inside the skin

Drug extraction from the skin: At the end of the permeation study, extracted drug from the skin was evaluated following a protocol described elsewhere.[2] The skin was removed from the Franz cell, cleaned with gauze soaked in a 0.05% solution of sodium dodecyl sulfate and washed in distilled water accurately. The permeation area of the skin was then excised, punctured with a needle, weighed, and drug contained therein was extracted with 1 mL of the corresponding receptor medium during 20 min of sonication. The resulting solutions were measured by HPLC, yielding the amount of drug extracted from the skin expressed in ($\mu g\ g^{-1}\ cm^{-2}$). Non-parametric Mann Whitney test statistical analyses were performed to compare drug retention from different formulations. [7]

Drug recovery experiments: A piece of skin from the same patient as in permeation experiments was immersed in 1 mL of a 21 µg/mL AEBSF·HCl solution, using as solvent the receptor medium used in release and skin permeation studies, and kept at 32°C for 27 hours. The skin piece was cleaned with gauze soaked in a 0.05% solution of sodium dodecyl sulfate and washed in distilled water accurately. Drug concentrations of both solutions "before immersion" and "after immersion" were determined using HPLC in order to know the amount of drug that can be retained within the skin. Skin pieces were punctured with a needle, and drug was extracted with 1 mL of the corresponding receptor solution using sonication, as performed in drug retention experiments. Concentrations of the drug extractions were determined using HPLC. The percentage of drug that can be recovered after being retained within skin was determined as follows:

Drug recovery (%) = drug extracted (µg) / drug retained (µg).

Drug retention inside the skin: The percentage of drug recovery was used for estimating the real amount of drug retained within skin during the skin permeation experiments.

HPLC determination

Concentrations of **AEBSF·HCl** were obtained by HPLC in a Waters 717 plus Autosampler, with a 600 Controller pump, equipped with a 2996 Photodiode Array Detector, using a 4 µm (3.9 mm x 150) Nova-Pack C18 column. The mobile phase consisted of acetonitrile:water (both with 0.07% of trifluoroacetic acid) 45:55, with a flow rate of 0.8 mL min^{-1}, setting a detection wavelength of 226 nm. Each sample had a run time of 4 min. The data were collected using Millennium32 version 4.0.0 software from Waters Corporation.

References

[1] L. Casal-Dujat, M. Rodrigues, A. Yagüe, A. C. Calpena, D. B. Amabilino, J. González-Linares, M. Borràs and L. Pérez-García, *Langmuir*, 2012, 28, 2368–2381.

[2] E. González-Mira, S. Nikolić, M. L. García, M. A. Egea, E. B. Souto and A. C. Calpena, *J. Pharm. Sci.*, 2011, 100, 242–51.

[3] G. Abrego, H. Alvarado, E. B. Souto, B. Guevara, L. H. Bellowa, A. Parra, A. Calpena and M. L. Garcia, *Eur. J. Pharm. Biopharm.*, 2015, 95, 261–270.

[4] M. Gibaldi and S. Feldman, *J. Pharm. Sci.*, 1967, 56, 1238–1242.

[5] Scientific Committee on Consumer Safety, *Eur. Comm.*, 2010, SCCS/1358, 1–14.

[6] OECD, Guidelines for the Testing of Chemicals, Section 4, Test No. 428: Skin Absorption: In Vitro Method, 2004.

[7] A. C. Williams, P. A. Cornwell and B. W. Barry, *Int. J. Pharm.*, 1992, 86, 69–77.

SUPPORTING RESULTS

Influence of drug concentration on gelation

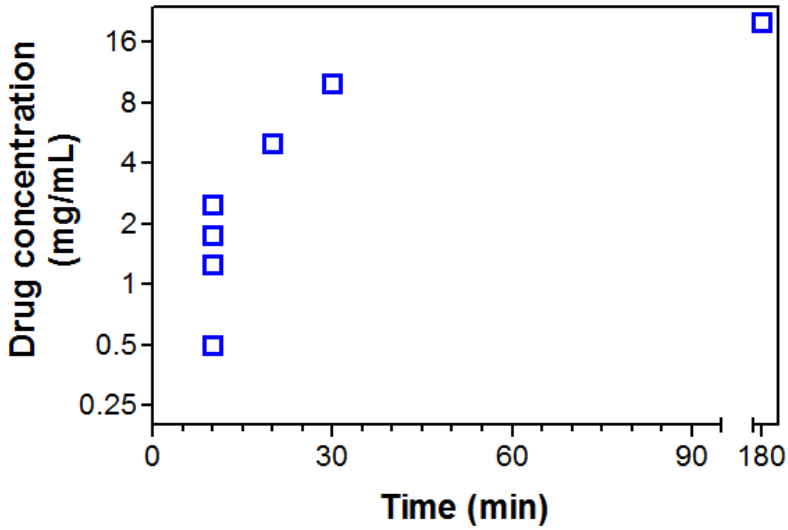

Figure S1. Gel formation time as a function of **AEBSF·HCl** concentration.

Rheology experiments

Table S1. Critical shear stress and G' values of gels **1·2Br** and **1·AEBSF**

Gel	G' at τ = 0.5 Pa (Pa) Frequency sweep tests[a]	Critical stress (Pa) [b]
1·2Br	1336	8.1
1·AEBSF	741	24.1

[a] Frequency sweep tests were performed at τ = 0.5 Pa for being within the viscoelastic region. [b] Shear stress experiments were performed at 1 Hz frequency.

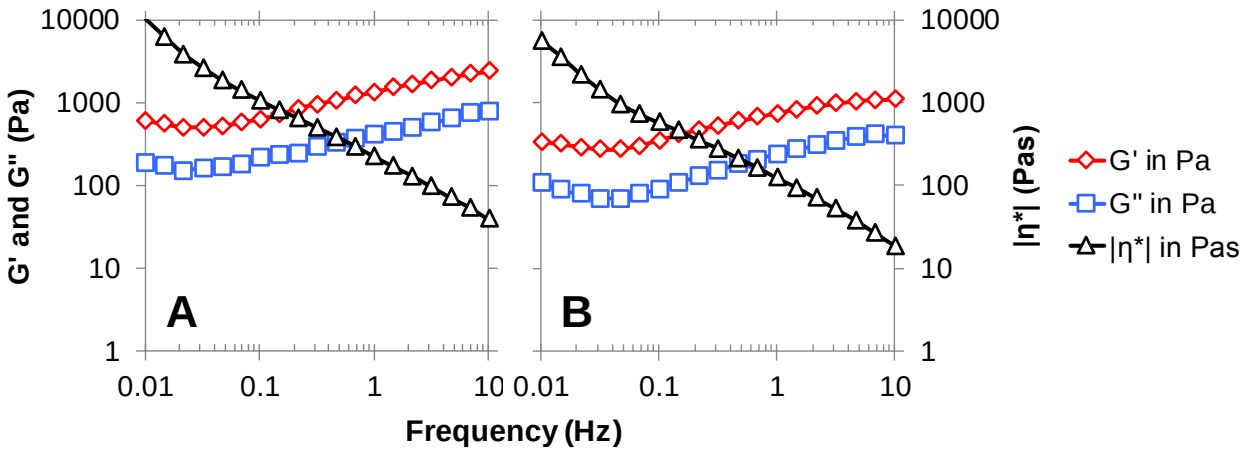

Figure S2. Rheograms of the oscillation sweep frequency test obtained for gels:

A) **1·2Br**, B) **1·AEBSF**.

Drug incorporation studies

Identical amounts of drug (8.28 µmol) were dissolved in deuterium oxide (0.75 mL) and put in two NMR tubes (A and B), and a spectrum of both was recorded (Record 1). Later on, a solution of gelator compound **1·2Br** (8.28 µmol) in deuterated methanol (0.75 mL) was added to tube B while the same volume of solvent without compound was added to tube A. Tubes were shaken, resulting in gel formation in tube B but not in tube A. The final concentration of **1·2Br** in tube B was 5 mg/mL. A spectrum of both tubes was recorded again (Record 2) and the intensity of the drug signals between Records 1 and 2 was compared. In both tubes, a decrease in the intensity of drug signals is expected in Record 2 when compared to Record 1 mainly due to the dilution generated by the addition of solvent. However, in tube B the decrease is higher because of some drug incorporation inside the fibres.

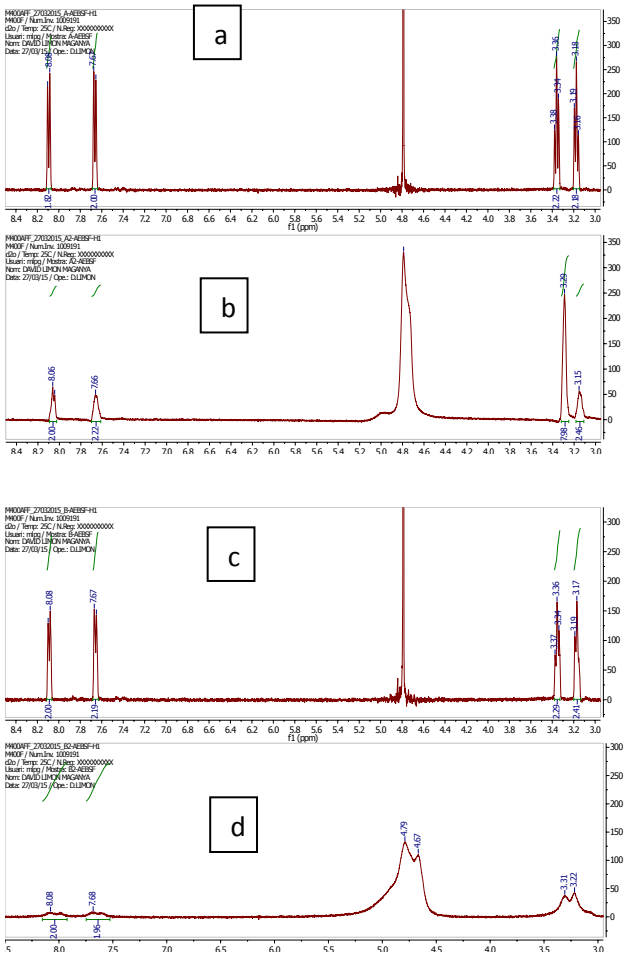

Figure S3. Incorporation of **AEBSF·HCl** in gel **1·2Br**.

a) Tube A, Record 1: **AEBSF·HCl** (8.28 µmol) in 0.75 mL of deuterium oxide.

b) Tube A, Record 2: after addition of 0.75 mL of deuterated methanol.

c) Tube B, Record 1: **AEBSF·HCl** (8.28 µmol) in 0.75mL of deuterium oxide.

d) Tube B, Record 2: after addition of **1·2Br** (8.28 µmol) in 0.75 mL of deuterated methanol.

Microscopy (SEM)

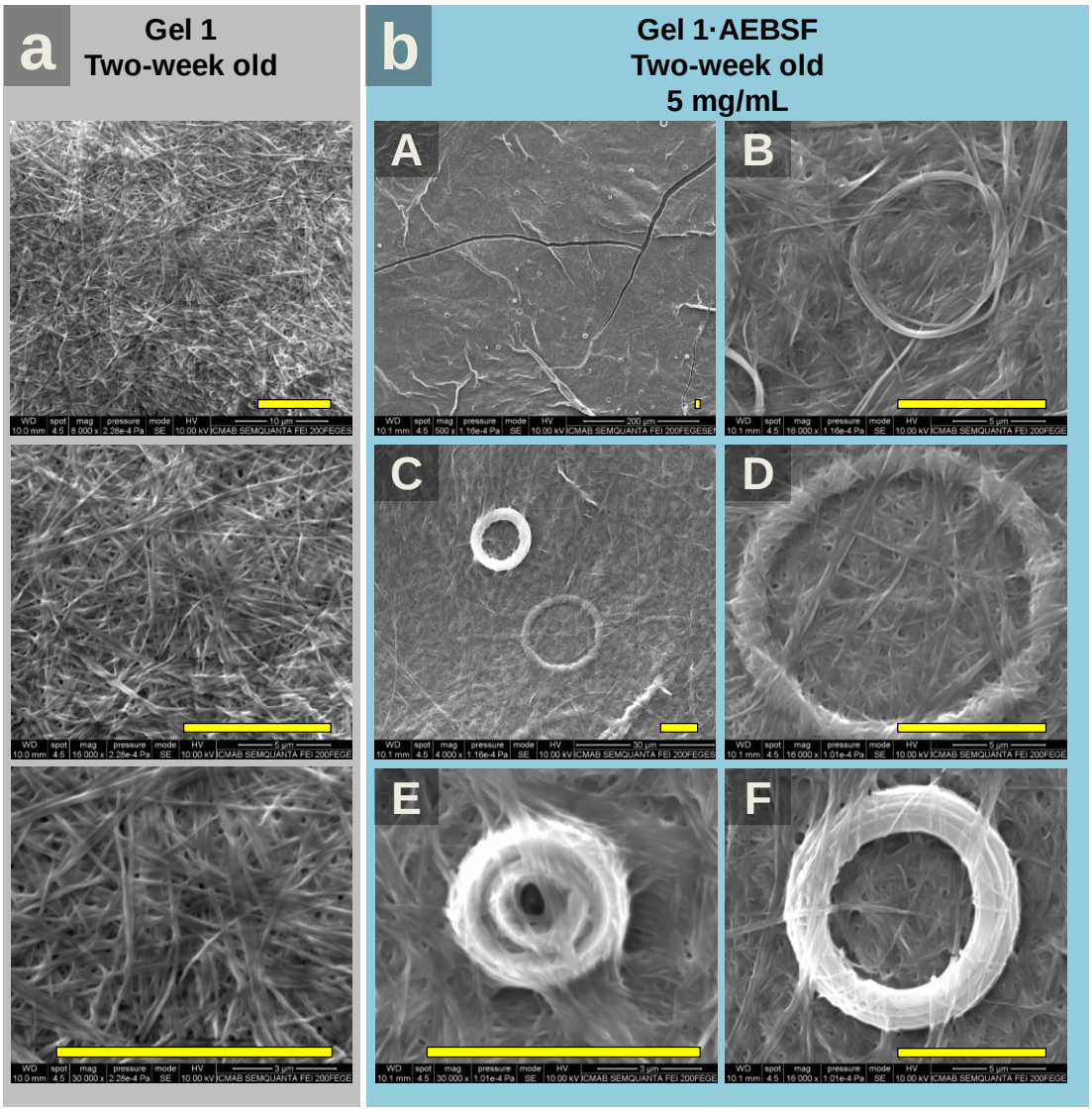

Figure S4. SEM micrographs of two-week old gels. a) Gel **1·2Br**. b) Gel **1·AEBSF** at a drug concentration of 5 mg/mL. Yellow scale bar represents 8 µm in all images.

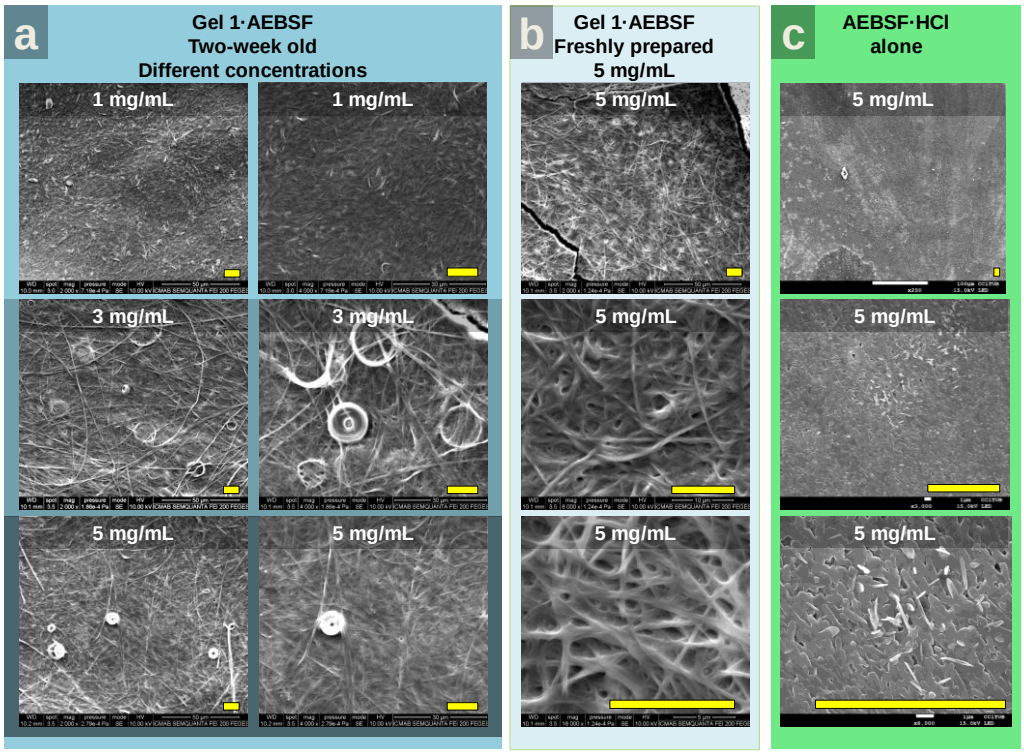

Figure S5. SEM images showing the influence of drug concentration and age of the gel on the structure of gel **1·AEBSF** fibres. a) Influence of the drug concentration in a two-week old gel. The increase in drug concentration induces the formation of coils. No drug precipitates are observed. b) Influence of the age in a 5 mg/mL drug concentration gel. In a freshly prepared gel, coils are still not formed, but fibres are twisted. No drug precipitates are observed. c) Precipitates of drug **AEBSF·HCl** alone, previously in a 5 mg/mL solution. Yellow scale bar represents 10 µm in all images.

Microscopy (EDX)

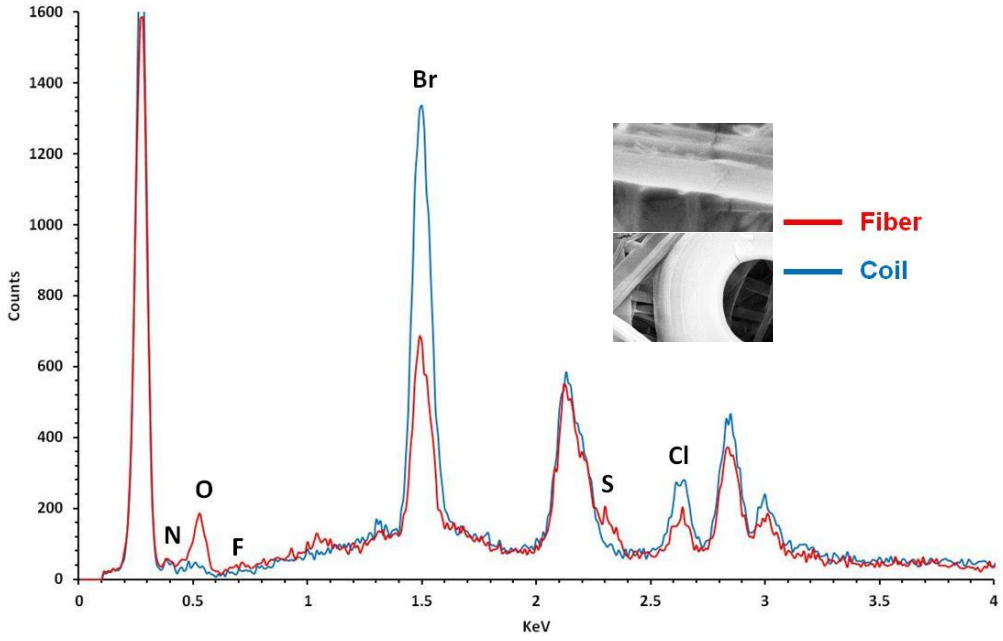

Figure S6. EDX spectra from a straight fibre and a coiled fibre of 3 mg/mL **1·AEBSF** gel. No sulphur or oxygen are observed in the coiled fibre, suggesting a loss of drug.

Calorimetric studies

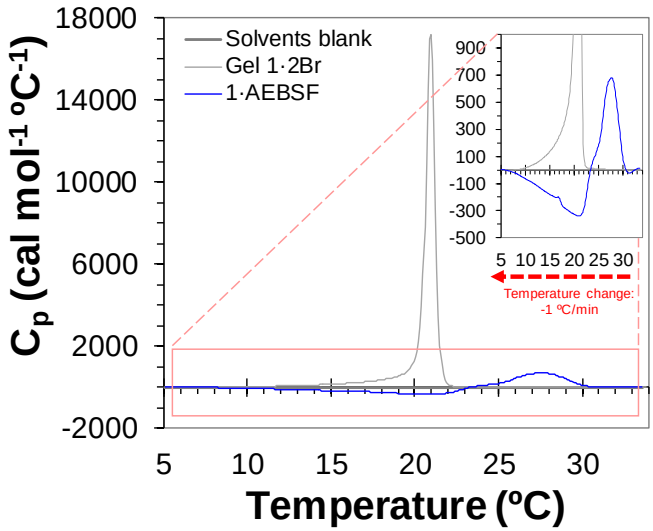

Figure S7. DSC thermogram plotting the heat capacity (C_p) of gel formation, which represents the speed of gelation, both from gel **1·2Br** and gel **1·AEBSF**. A magnification is shown in the inset. Temperature was decreased at a speed of 1 °C min^{-1}.

Table S2. Influence of **AEBSF·HCl** addition on gel formation time and temperature.

Gel	T_{onset} [a] (ºC)	T_{max} [b] (ºC)	T_{offset} [c] (ºC)	t_{gel} [d] (min)
1·2Br (without drug)	21.7	20.8	19.4	3.3
1·AEBSF (exo)	30.5	27.8	23.2	7.3
1·AEBSF (endo)[e]	23.2	21.2	5.9	17.3

[a]Temperature at which the gelling starts. [b]Temperature at which the gelling occurs at the highest speed. [c]Temperature at which gelling speed stops changing significantly. [d]Time required for gel formation. [e]Gel **1·AEBSF** showed both and exothermic and an endothermic peak.

The thermoreversibility of gel **1·AEBSF** is proven by performing various heating-cooling cycles, showing a decrease in C_p values, and suggesting that the heating of the gel to 35 ºC macroscopically melts the gel, but leaves some gel nucleation points unmelted, which facilitates the subsequent gelation.

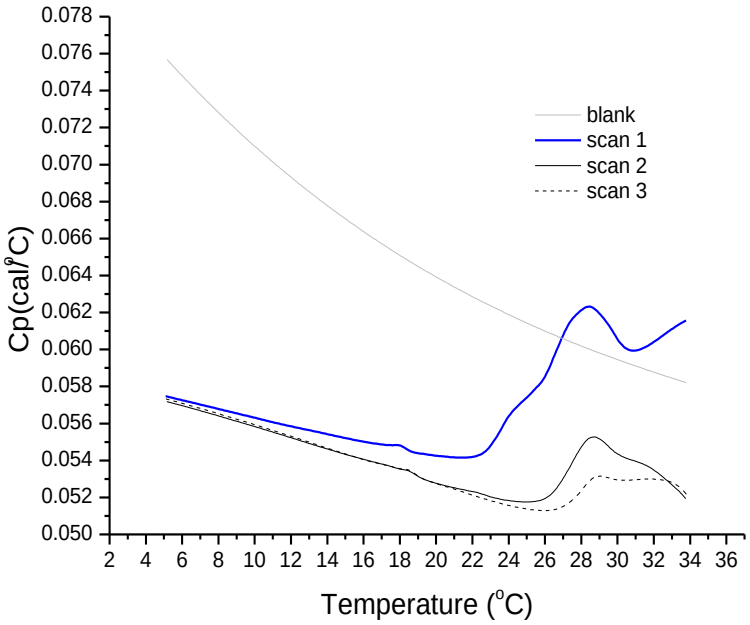

Figure S8. Thermograms of gel **1·AEBSF** formation. Different cycles were performed to prove thermoreversibility.

Drug release

In Figure 4 in the main article. Drug release is shown to follow a *One phase exponential association model* [$Y = Y_{max} (1 – e^{-K X})$], where Y represents the cumulative percentage of drug released at a certain time, Y_{max} is the maximum amount of drug that can be released, K is the rate of release (h^{-1}) and X is time (h). Degradation follows a *One phase exponential decay* model, described by the equation: [$Y = Span \cdot e^{-KX} + Plateau$], where Y is the amount of drug present in the receptor chamber at a certain time (%), (Span+Plateau) is the theoretical amount of drug at time zero (%), K is the speed of degradation (h^{-1}), and Plateau is the amount of drug remaining at an infinite time (%).

Table S3. Drug release and degradation parameters of **AEBSF** when released from gel **1·2Br**. Values represent the Means ± one standard deviation (n=3).

	Drug release	Drug degradation
Y_{max} (%)[a]	91.92 ± 3.23	
K (h^{-1})[b]	0.146 ± 0.013	0.013 ± 0.002
Span (%)[c]		91.43 ± 2.51
Plateau (%)[e]		7.28 ± 3.42
Half-life (h)[f]		55.57
R^2	0.9967	0.9970

[a]Maximum drug release (%). [b]Release/degradation speed rate (h^{-1}). [c]Theoretical amount of drug at time zero in degradation model (%) [e]Drug remaining at infinite time [f]Time for the degradation of 50% of drug remaining in receptor chamber.

Skin permeation

Table S4. Skin permeation parameters of **AEBSF** from gel **1·2Br**.

Gel	**1·AEBSF** (5 mg/mL)
A_{18} (μg/cm^2)[a]	40.64 (40.62 - 72.63)
A_{21} (μg/cm^2)[a]	45.88 (40.40 - 79.43)
A_{24} (μg/cm^2)[a]	72.17 (49.20 - 95.59)
A_{27} (μg/cm^2)[a]	80.72 (66.40 - 122.05)
J (μg/h·cm^2) [b]	5.27 (3.01 – 5.71)
T_{lag} (h)[c]	6.59 (6.44 – 11.47)
$K_p \cdot 10^3$ (cm/h)[d]	1.05 (0.60 – 1.14)
A_s (μg/g·cm^2)[e]	90.59 (40.31 - 107.17)
Percentage of recovery (%)[f]	2.6%
A_s corr. (μg/g·cm^2)[g]	3484.20 (1550.38 – 4121.92)

[a]A18, A21, A24, A27 is the cumulative amount of drug permeated after 18, 21, 24 and 27 hours, respectively. [b]J represents the permeation flux of drug through the skin (μg/h·cm^2). [c]T_{lag} represents the time the drug takes to completely cross the skin to the receptor chamber. [d]K_p is the Permeability coefficient (cm/h) [e]A_s is the amount of drug extracted after the experiment per gram and square centimeter of skin (μg/g·cm^2). [f]Percentage of drug that can be extracted out of all the drug retained inside the skin. [g]Total estimated amount of drug retained inside the skin according to the percentage of recovery. Values represent the Median and range.

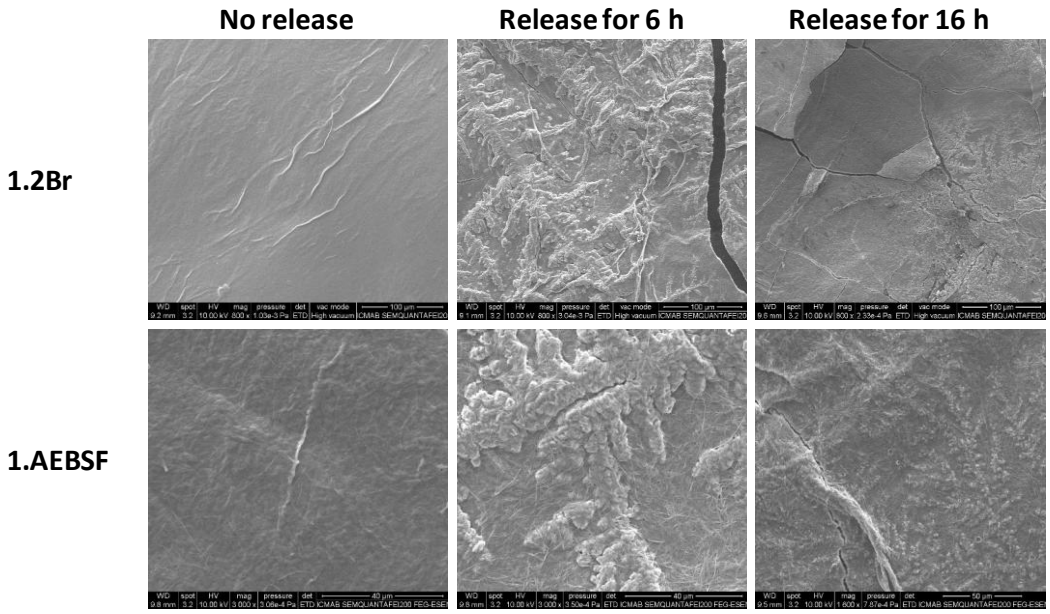

Figure S9. SEM images showing the influence of drug release on the morphology of the fibres. Image are shown for the fresh gels **1·2Br** and **1·AEBSF**, at 6 hours under release conditions and at 16 hours under release conditions. The lumpy material for the samples held under release conditions arises from the buffer used under those conditions.

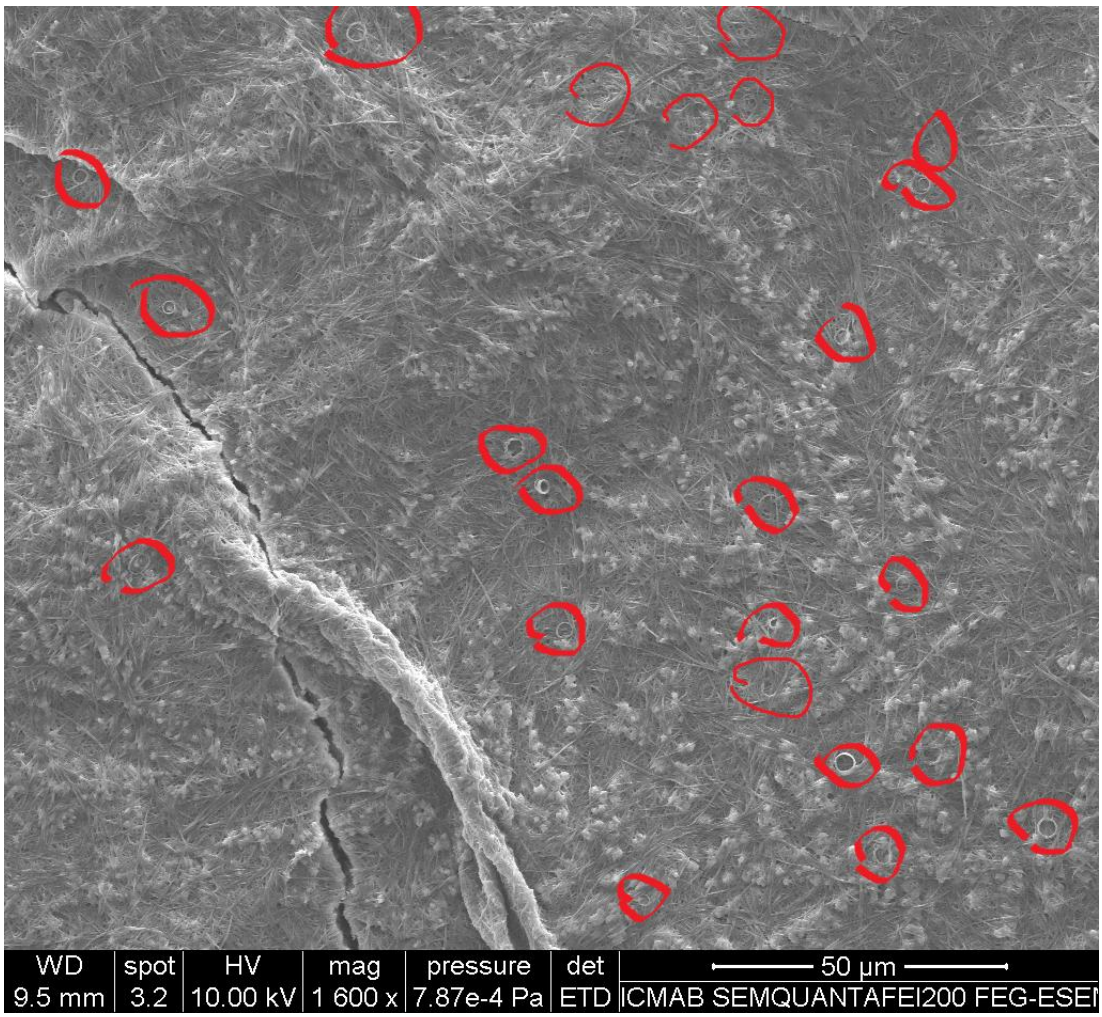

Figure S10. SEM image of **1·AEBSF** after 16 hours under release conditions with the coil structures circled.

Powder X-ray Diffraction

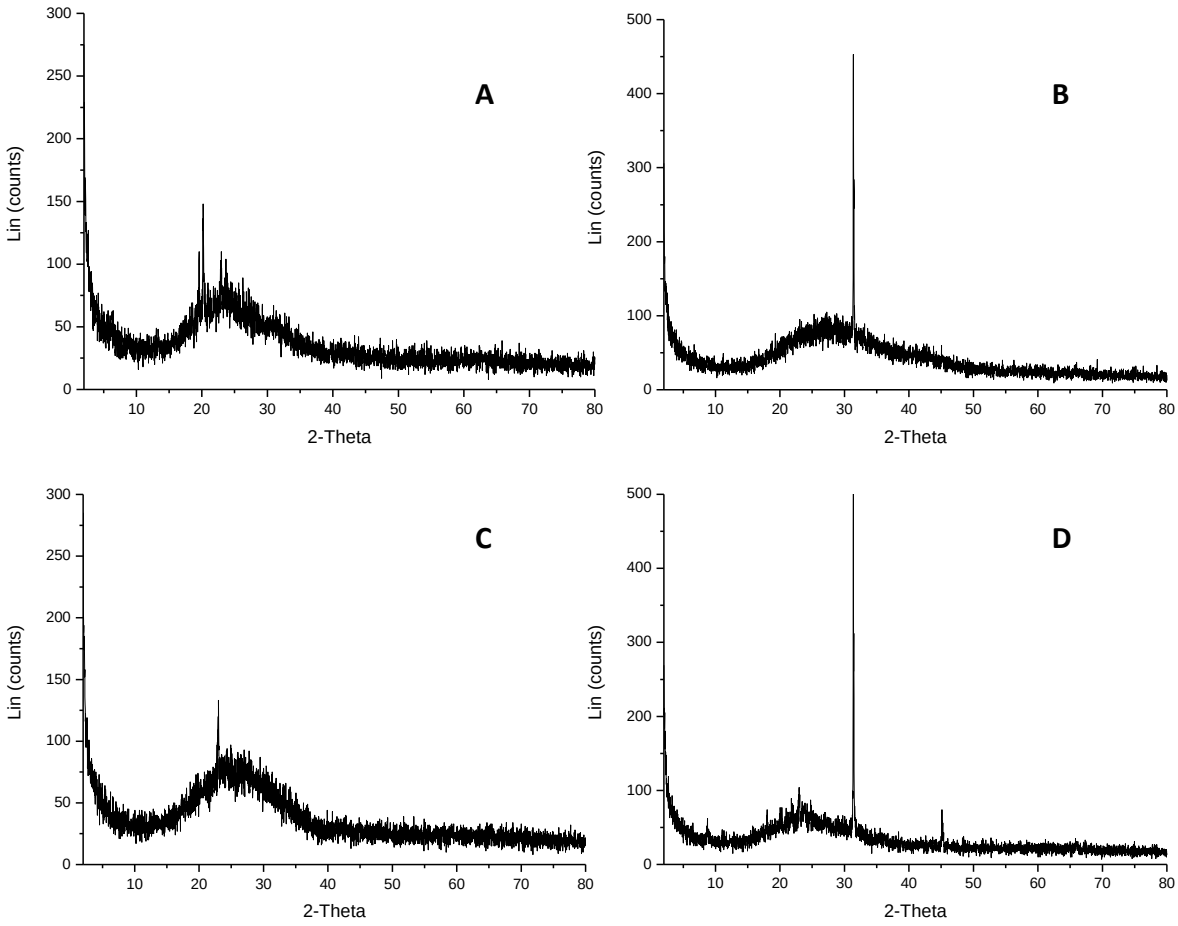

Figure S11. Powder X-ray diffractograms of a fresh gel with drug **1·AEBSF** (A) and after 16h of release (B); an aged gel (2 weeks) with drug (C) and after 16h of release

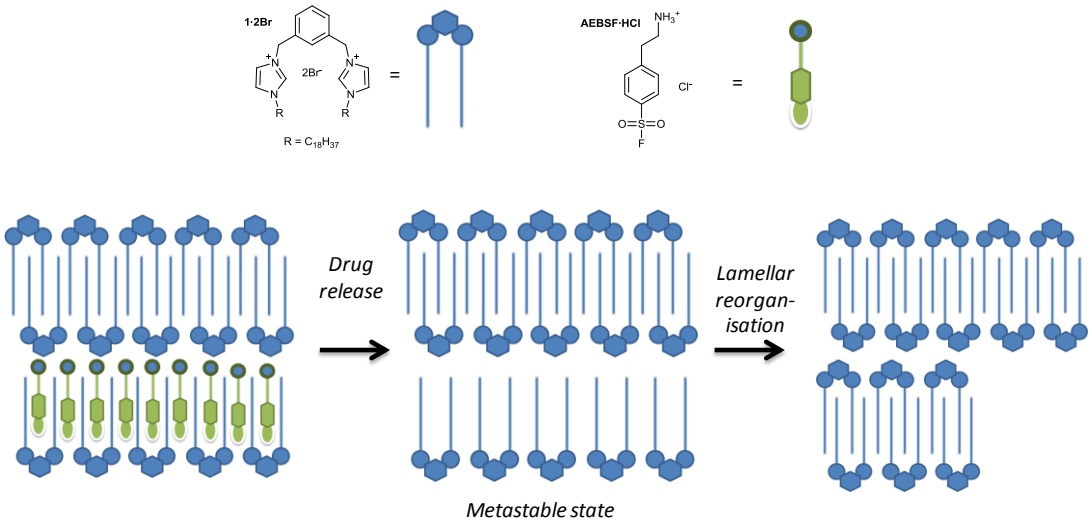

Figure S12. A possible explanation for the generation of stress - and resulting curvature - upon release of the drug from the composite gel. Counter-ions (the anions to both gelator and drug) are not shown in the cartoon but are believed to be located between the lamellae in contact with the cations.